Secondary circulation associated with a shelfbreak front

John A. Barth, Darek Bogucki, Stephen D. Pierce, and P. Michael Kosro

College of Oceanic & Atmospheric Sciences, Oregon State University, Corvallis, Oregon

Abstract. Evidence for secondary circulation associated with a shelfbreak front is obtained from a high-resolution, cross-shelf section of hydrographic, optical and velocity fields. Convergence in the bottom boundary layer on the inshore side of the front and subsequent upwelling into the interior is evident by a mid-water region of suspended bottom material emanating from the foot of the front and extending to within 35 m of the surface, 80 m above bottom. Downwelling on the offshore side of the front in the upper water column is inferred from a 20-m downward bend of the subsurface phytoplankton layer. These observations are in agreement with recent model predictions for secondary circulation near an idealized shelfbreak front. Convergence in measured cross-shelf velocity at the foot of the front is consistent with upwelling of bottom material detected there. An estimate of 9 ± 2 m day^{-1} of upwelling on the inshore side of the shelfbreak front is obtained, implying a transit time from the bottom to the surface of 10-16 days.

Introduction

In the Middle Atlantic Bight (MAB), a shelfbreak front is often found separating cold, fresh shelf water from warm, saline slope water offshore. The associated westward alongshore jet, the primary circulation, is an order of magnitude stronger than any secondary circulation that may occur in a cross-shelf, vertical plane. This disparity makes measurement of the secondary circulation challenging. Another way to "measure" the secondary circulation is to infer it from distributions of passive tracers present in the flow field. In this paper, two naturally occurring tracers, phytoplankton and suspended bottom material, are used to infer the secondary circulation associated with the shelfbreak front in the MAB.

The physical, optical and velocity distributions presented here and the secondary circulation inferred from them will be compared with idealized model predictions. Gawarkiewicz and Chapman (1992) and Chapman and Lentz (1994) (hereafter CL) have presented models for the secondary circulation associated with an idealized coastal density front. To reach the steady

state predicted by CL, offshore buoyancy flux in the bottom boundary layer (BBL) occurs until the foot of the front is deep enough such that the vertical shear within the front (in thermal wind balance with the relatively time-independent, cross-shelf density gradient) causes a reversal in the near-bottom cross-shelf flow. This results in convergence in the BBL on the inshore side of the density front and upwelling into the interior. Near the surface on the offshore side of the front, convergence also occurs but here leads to downwelling.

Data

Vertical profiles of water properties were made across the continental shelf and slope south of Cape Cod, Massachusetts using instruments aboard SeaSoar, a towed, undulating measurement platform. The vehicle cycled through the water column between the surface and to within 5-10 m of the bottom while being towed at 7-8 knots (3.6-4.1 m s^{-1}). Complete cycles to 105(55) m were accomplished in 210(75) s at the offshore (onshore) end of a cross-shelf section; horizontal separation at the surface and bottom of the sawtooth-shaped SeaSoar trace was 800(300) m. From August 14 to September 1, 1996, repeated cross-shelf sections were made at several alongshore locations near 40.5°N, 70.5°W.

Temperature, conductivity and pressure were measured at 24 Hz using a Seabird 911+ instrument with the sensors mounted pointing forward through SeaSoar's nose. Salinity and density were obtained following procedures described in Barth et al. (1998) and vertical sections were made by averaging over 1.2 km horizontally and 2-db in the vertical.

Light attenuation and absorption at nine wavelengths were measured at 6 Hz using a WETLabs ac9 instrument mounted on top of SeaSoar. Water pumped through the optical measurement tubes without filtering was obtained from an inlet adjacent to the Seabird sensors in the nose of SeaSoar. A time lag was applied to the optical data to align it with the hydrographic data so that light absorption could be corrected for temperature dependence. Vertical sections were made from 1-sec averaged data.

Vertical profiles of velocity were obtained using an RDInstruments 300-kHz, hull-mounted acoustic Doppler current profiler (ADCP). The ADCP had vertical bins and pulse lengths of 4 m, an ensemble averaging time of 2.5 min, and a depth range of 10-200 m. Details of the ADCP data processing follow those described by Pierce
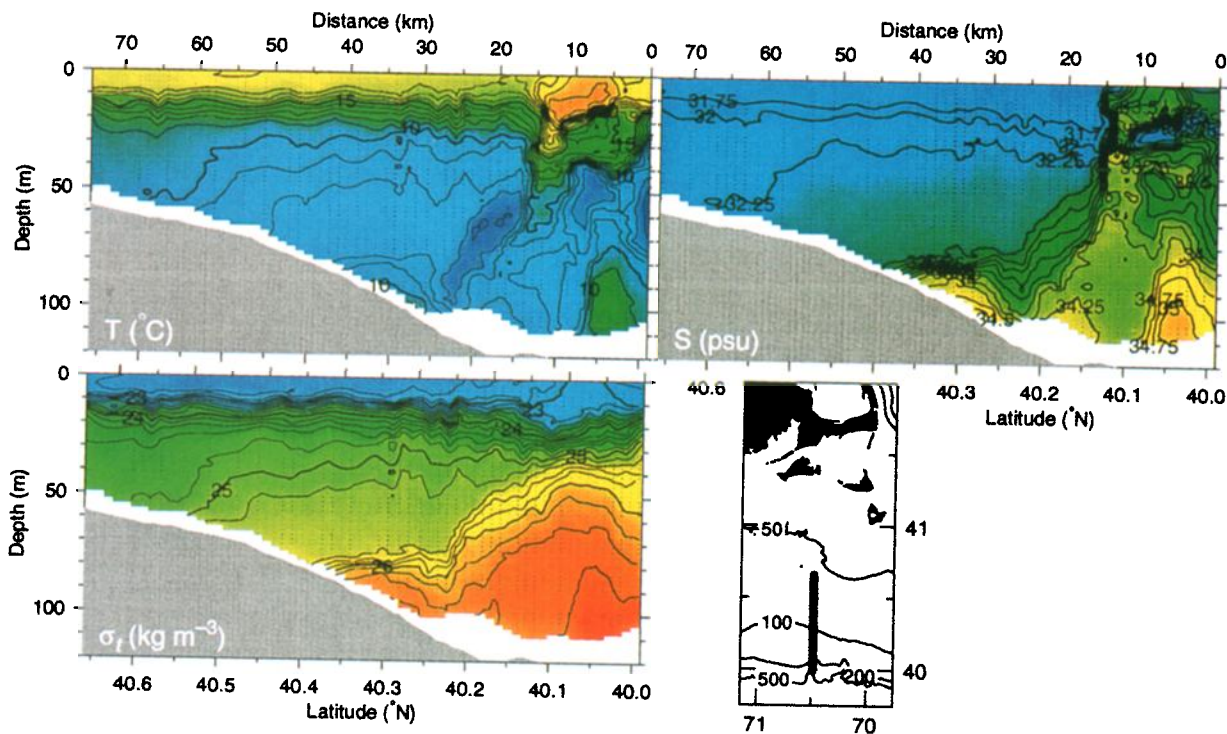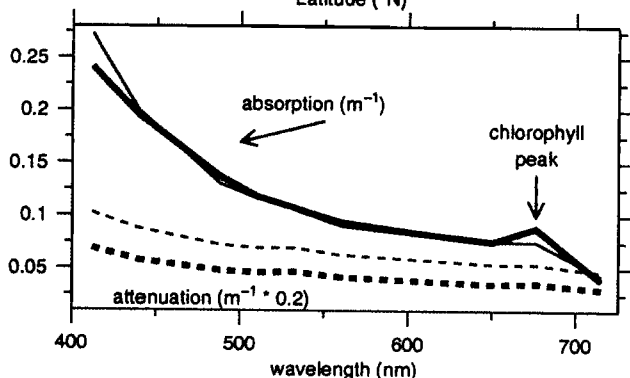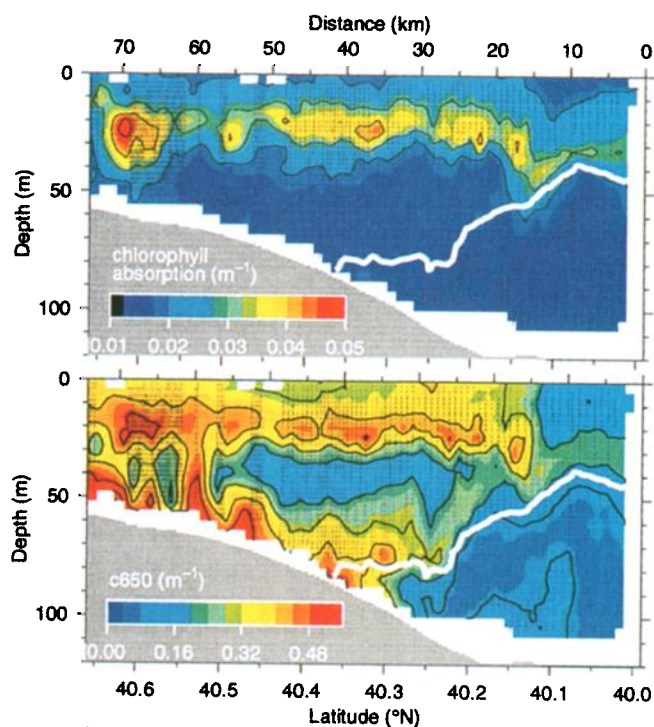
Figure 1. Cross-shelf sections of temperature, salinity and density along 70.48°W from 13:01 to 19:35 UTC on August 21, 1996. Gridded data locations are shown as light dots. The location of the cross-shelf section is indicated by a thick line on the map.

et al. (1997). Short-term inherent random errors for an ensemble are at most 0.015 m s^{-1} and estimated rms errors in absolute velocity are 0.01 m s^{-1} while bottom tracking (water depth < 200 m) and 0.03 m s^{-1} when using differential GPS navigation. The ADCP velocities were detided by removing depth-averaged tidal currents estimated from harmonic analysis following Candela *et al.* (1992). M2 current amplitudes vary between 0.02 m s^{-1} over the slope to 0.15 m s^{-1} near the shallow end of the cross-shelf transect.

Results

Vertical sections of temperature, salinity and density measured across the continental shelf and slope are shown in Figure 1. A warm surface layer exists over the entire section separated from colder water below by

Figure 2. Cross-shelf sections of chlorophyll absorption and 650-nm light attenuation measured with a nine-wavelength absorption and attenuation instrument on the towed, undulating vehicle SeaSoar along 70.48°W from 13:01 to 19:35 UTC on August 21, 1996. The thick white curve is the $\sigma_t = 25.8$ kg m^{-3} isopycnal; data locations are indicated by light dots. On the bottom are spectra of light absorption (solid curves) and attenuation (dashed curves) from a depth of 50 m at 40.13°N (thick curves) and at 40.21°N (thin curves).

a strong thermocline between 10 and 30 m. The thermocline bends downward near 40.1°N so that a region of warm water separates cold water inshore, the "cold pool", from that found offshore in the mid-water column. Warm, salty slope water is present offshore at depth. The salinity field is relatively uniform over the shelf, separated from offshore water by a strong surface-to-bottom front located between 40.1 and 40.35°N. A strong pycnocline 10-20 m above bottom (mab) is found where the salinity front intersects the bottom at 85 m depth; this defines the "foot" of the shelfbreak front. In the upper half of the water column associated with the salinity front are several mesoscale (5-10 km) features. The density field shows a strong pycnocline between 10 and 30 m over the region due mostly to temperature over the shelf and to both temperature and salinity offshore. The shelfbreak density front rises from the seafloor near 40.35°N to within 35 m of the surface before bending down offshore. This bending down offshore may be due to horizontal meandering of the front.

Vertical sections of light absorption in the chlorophyll band, an indicator of chlorophyll concentration, and light attenuation at 650 nm are shown in Figure 2. Chlorophyll absorption is obtained by computing the area under the 676-nm peak above the background absorption level: a676 − (a650 + a715)/2. Chlorophyll concentration is high near the base of the pycnocline across the entire shelf but bends down abruptly (from 30 to 50 m) in the region of the shelfbreak front (40.1°N). Offshore of this region of deep chlorophyll, elevated values are found following the density surface defining the shelfbreak front ($\sigma_t = 25.8$ kg m^{-3}). Light attenuation at 650 nm, a measure of the total suspended particulate matter, is elevated within the chlorophyll features just described, but is also high in a bottom nepheloid layer. A warm, salty mesoscale surface lens near 40.075°N is clear compared with the rest of the surface waters; low light attenuation here is consistent with low chlorophyll. Offshore at depth the water is clear and there is relatively less light attenuation in the mid-water column over the shelf between the pycnocline chlorophyll maximum and the BBL. A noticeable feature is the tongue of high light attenuation extending up through the water column from the foot of the shelfbreak front (40.35°N), along the inshore side of the frontal boundary ($\sigma_t = 25.8$ kg m^{-3}) and reaching to within 35 m of the surface just inshore of the downward dipping chlorophyll maximum. Between approximately 35 and 50 m, the two maxima, chlorophyll offshore and light attenuation inshore, are separated horizontally. Also shown in Figure 2 are spectra of light absorption and attenuation at 50 m from within the two maxima. The absorption spectra have been scaled so that a650 is the same in both samples to highlight differences in the 676-nm chlorophyll peaks. The material in the offshore sample is high in chlorophyll and has lower light attenuation at all wavelengths than that found in the inshore sample, which is presumably rich in suspended sediment.

Vertical sections of ADCP velocity show a strong, surface-intensified alongshore jet in thermal wind balance with the sloping shelfbreak front (Figure 3). Cross-shelf velocities show offshore flow ($v < 0$) near the foot of the front (40.3°N) with a region of onshore flow near the bottom (40.15°N) just offshore. The implied convergence near the foot of the front (40.2-40.25°N) is evident in a plot of the cross-shelf derivative of cross-shelf velocity, i.e. horizontal divergence assuming alongshore uniformity. There is also convergence in the mid-water column near 40.1-40.15°N and divergence in the upper-water column near 40.2-40.25°N and at depth offshore of the front (40.05-40.1°N). Here the positive cross-shelf direction is due north, which maximizes the alignment between the coordinate system and the front/jet, thus yielding the strongest secondary circulation signal.
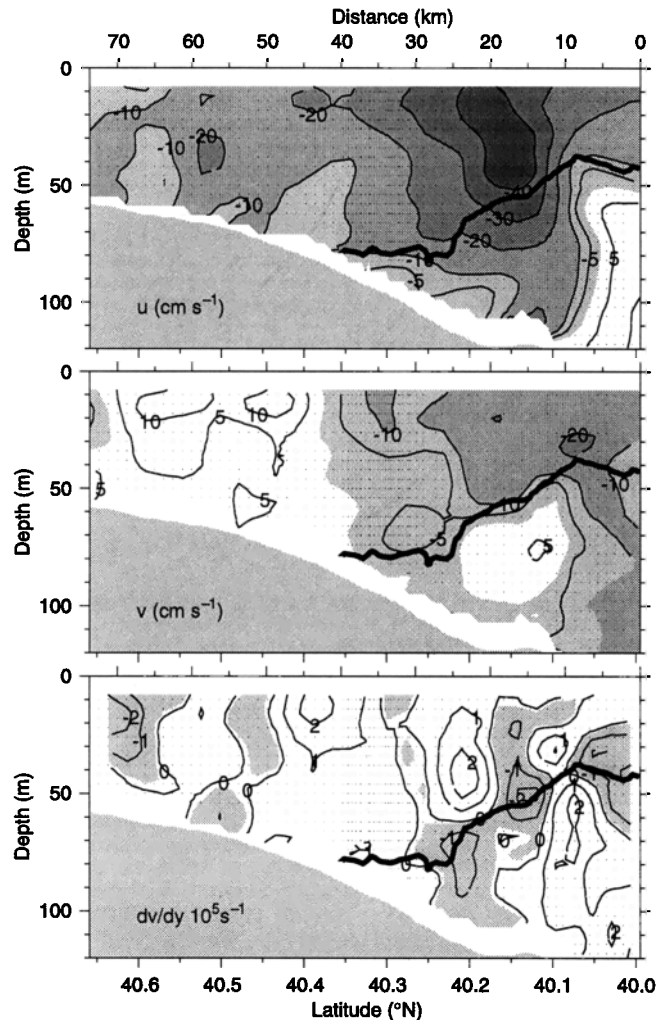

Figure 3. Cross-shelf sections of alongshore (u) and cross-shelf (v) velocity, measured with a shipboard acoustic Doppler current profiler, and the cross-shelf derivative of v (dv/dy). Regions with negative values are shaded and the thick curve is the $\sigma_t = 25.8$ kg m^{-3} isopycnal; gridded data locations are indicated by light dots.

Discussion

The region of elevated light attenuation emanating from the BBL and extending upward through the water column along the inshore side of the shelfbreak front is consistent with model predictions of Gawarkiewicz and Chapman (1992) and CL. In CL, neutrally buoyant particles released near the bottom and shoreward of the density front were advected up along the frontal boundary. The same pattern is observed here as evident by upwelled bottom material.

The downward bend from 30 to 50 m of the subsurface chlorophyll maximum associated with the shelfbreak front may indicate downwelling. This pattern is consistent with the downwelling predicted by CL in the upper part of the water column near the offshore side of the shelfbreak front. In fact, the four maxima visible in ADCP divergence (Figure 3), divergence above convergence on the inshore side of the front, convergence above divergence on the offshore side of the front, are consistent with CL's results.

Assuming that near-bottom cross-shelf convergence is balanced by upwelling, the ADCP convergence field (Figure 3) can be integrated over a region 30 mab and 15 km across to yield an upwelling estimate of 9 ± 2 m day^{-1}. Thus, a water parcel could travel from the bottom along the front to the surface (a distance of 115 m) in 10-16 days.

Two additional long, cross-shelf SeaSoar/ADCP sections were obtained to the west of the data presented here. A section 13 km to the west shows a similar bending down of the chlorophyll maximum where the shelfbreak front approaches the surface. A region of elevated light attenuation at depth is found following the inshore side of the front and separating clearer water above and below. This region extends 30 km along the sloping front and is up to 20 m in height. A section 25 km to the west shows a similar downward turn in the upper-water column chlorophyll maximum, but only a small region (< 5 km wide, 20 m high) of elevated attenuation near the foot of the front. Therefore, the implied convergence and upwelling near the foot of the front is occurring over at least 25 km in the alongfront direction, but there is alongfront variation in either the strength of the circulation or the efficiency with which it resuspends bottom material.

Complimentary evidence for convergence near the foot of the shelfbreak front and subsequent upwelling was found by Houghton and Visbeck (1998) using a purposeful dye release in the BBL. They estimate an equivalent upwelling velocity of 4-7 m day^{-1}, consistent with results presented here.

Conclusions

By using a high-resolution, cross-shelf section of physical, optical and velocity fields from the Middle At-

lantic Bight, the secondary circulation associated with a shelfbreak front has been documented. Convergence near the foot of the shelfbreak front and subsequent upwelling into the interior and downwelling on the offshore side of the front in the upper part of the water column were established from optical property distributions. Both elements of this secondary circulation are consistent with idealized model predictions. Cross-shelf velocities measured with shipboard ADCP were shown to be consistent with the convergence implied by the distribution of suspended bottom material. By integrating the measured divergence fields, an estimate of 9 ± 2 m day^{-1} of upwelling was made, implying a transit time from the seafloor to the surface of 10-16 days. This secondary circulation has important implications for the biogeochemistry of shelfbreak fronts through upwelling of nutrients into the euphotic zone and concentration of material on the offshore side of the front.

References

Barth, J. A., S. D. Pierce and R. L. Smith, A separating coastal upwelling jet at Cape Blanco, Oregon and its connection to the California Current System, Deep-Sea Res., in press, 1998.

Candela, R. C. Beardsley and R. Limeburner, Separation of tidal and subtidal currents in ship-mounted acoustic Doppler current profiler observations, J. Geophys. Res., 97, 769–788, 1992.

Chapman, D. C. and S. J. Lentz, Trapping of a coastal density front by the bottom boundary layer, J. Phys. Oceanogr., 24, 1464–1479, 1994.

Gawarkiewicz, G. and D. C. Chapman, The role of stratification in the formation and maintenance of shelfbreak fronts, J. Phys. Oceanogr., 22, 753–772, 1992.

Houghton, R. W. and M. Visbeck, Upwelling and convergence in the Middle Atlantic Bight shelfbreak front, Geophys. Res. Lett., in this issue, 1998.

Pierce, S. D., J. A. Barth and R. L. Smith, Acoustic Doppler Current Profiler observations during the Coastal Jet Separation project on R/V Wecoma, 17-27 August 1995, Data Report 166, Ref. 97-4, College of Oceanic and Atmospheric Sciences, Oregon State University, 1997.

John A. Barth, Darek Bogucki, Stephen D. Pierce and P. Michael Kosro, College of Oceanic & Atmospheric Sciences, Oregon State University, Corvallis, OR 97331-5503. (e-mail: barth@oce.orst.edu)